Probing the Nature of Higgs Physics and Electroweak Symmetry Breaking with Results from the LHC

Alexei Raspereza[1], *Peter Schleper*[2], *Kerstin Tackmann*[1,2], *Georg Weiglein*[1]

[1]DESY, Hamburg, Germany
[2]Institut für Experimentalphysik, Universität Hamburg, Germany

DOI: http://dx.doi.org/10.3204/PUBDB-2018-00782/B9

The discovery of a Higgs signal at the LHC marks the beginning of a new era of particle physics. The prime goal now is to identify the underlying physics of the new state and to determine the mechanism of electroweak symmetry breaking. Some of the results obtained in this project are highlighted, covering both the period before and after the discovery. In particular, the properties of the new state have been investigated in close cooperation between experiment and theory and the possible interpretations of the observed signal have been analysed. Confronting the experimental results on the signal as well as from the search limits with model predictions, the resulting constraints on the parameter space of different models and their phenomenological implications have been demonstrated.*

1 Introduction

Identifying the physics that is responsible for providing elementary particles with the property of mass is one of the key issues in the quest for a better understanding of the fundamental interactions of nature. Within the present experimental and theoretical uncertainties the properties of the signal that was detected in the Higgs searches at the LHC are compatible with the predictions of the Standard Model (SM) of particle physics, but also with a wide variety of other possibilities, corresponding to very different underlying physics.

In this project the nature of Higgs physics and electroweak symmetry breaking has been probed in a joint effort between experiment and theory. In the following a brief account of some of the achieved results is given, comprising Higgs searches, property determinations, appropriate model predictions, as well as the discrimination between different interpretations of the experimental results.

*Contribution to "Particles, String and the Early Universe – Research Results of the Collaborative Research Centre SFB 676 in Hamburg".

2 Theoretical studies preceding the Higgs boson discovery

2.1 Light NMSSM Higgs bosons in SUSY cascade decays at the LHC

An interesting feature of the next-to-minimal supersymmetric extension of the Standard Model (NMSSM) is that one or more Higgs bosons may be comparably light ($M_{H_i} < M_Z$) without being in conflict with current experimental bounds. Due to a large singlet component, their direct production in standard channels at the Large Hadron Collider (LHC) is suppressed. In Ref. [1] good prospects for observing such a light Higgs boson in decays of heavy supersymmetric (SUSY) particles at the LHC were demonstrated.

Considering an example scenario with 20 GeV $< M_{H_1} < M_Z$, it was shown that a large fraction of cascade decays of gluinos and squarks would involve the production of at least one Higgs boson. Performing a Monte Carlo analysis at the level of fast detector simulation, it was demonstrated how the Higgs signal can be separated from the main backgrounds, see Fig. 1, where the simulation has been done for SUSY scales of $M_{\rm SUSY} = 750$ GeV (left column) and $M_{\rm SUSY} = 1$ TeV (right column). Besides the SM $t\bar{t}$ background also SUSY background from other SUSY processes has been taken into account. The impact of various kinematical variables on discriminating between the inclusive SUSY signal (including events both with and without a Higgs boson in the cascade) and the SM background from $t\bar{t}$ production has been investigated. A set of simple cuts has been devised that turned out to be efficient for establishing the inclusive SUSY signal. It should be noted that no specific knowledge about the background from SUSY background from events without a Higgs in the cascades was assumed. Accordingly, besides favoring events containing the light H_1 by selecting the combination minimizing $\Delta R(bb)$ in configurations with multiple b-jets, no particular cuts for suppressing the SUSY background have been applied.

It was pointed out in Ref. [1] that the analysis of the resulting $b\bar{b}$ mass spectrum according to Fig. 1 opened up an opportunity for the discovery of a light Higgs boson already with 5 fb^{-1} of LHC data at 7 TeV. In the considered scenario with rather light SUSY particles a statistical significance for the H_1 mass peak of $S/\sqrt{B} \approx 4$ was found for $M_{\rm SUSY} = 1$ TeV at $\sqrt{s} = 7$ TeV (the gluino mass parameter was set to 1 TeV), which increased to $S/\sqrt{B} \approx 8$ for $M_{\rm SUSY} = 750$ GeV at 7 TeV and reached a level of almost 30 for both values of $M_{\rm SUSY}$ at 14 TeV with the very modest integrated luminosity of just 5 fb^{-1} for LHC running both at 7 TeV and 14 TeV. The presented results are rather insensitive to the precise value of M_{H_1}. Since the production relies on the decay of heavier SUSY states, with branching ratios largely independent of M_{H_1}, the Higgs production rates remain similar for the whole mass range $M_{H_1} < M_Z$.

The observation of a light Higgs boson in this channel would give direct access to the Yukawa coupling of the Higgs state to bottom quarks. While compared to the experimental situation that was analysed in Ref. [1] the limits from SUSY searches have meanwhile become much stronger, there is still ample room for one or more light Higgs bosons with suppressed couplings to gauge bosons, as will be discussed in more detail below.

The phenomenological investigation carried out in Ref. [1] triggered an experimental activity that is described in Sec. 6.5 below. It resulted in the CMS analysis of Ref. [2].

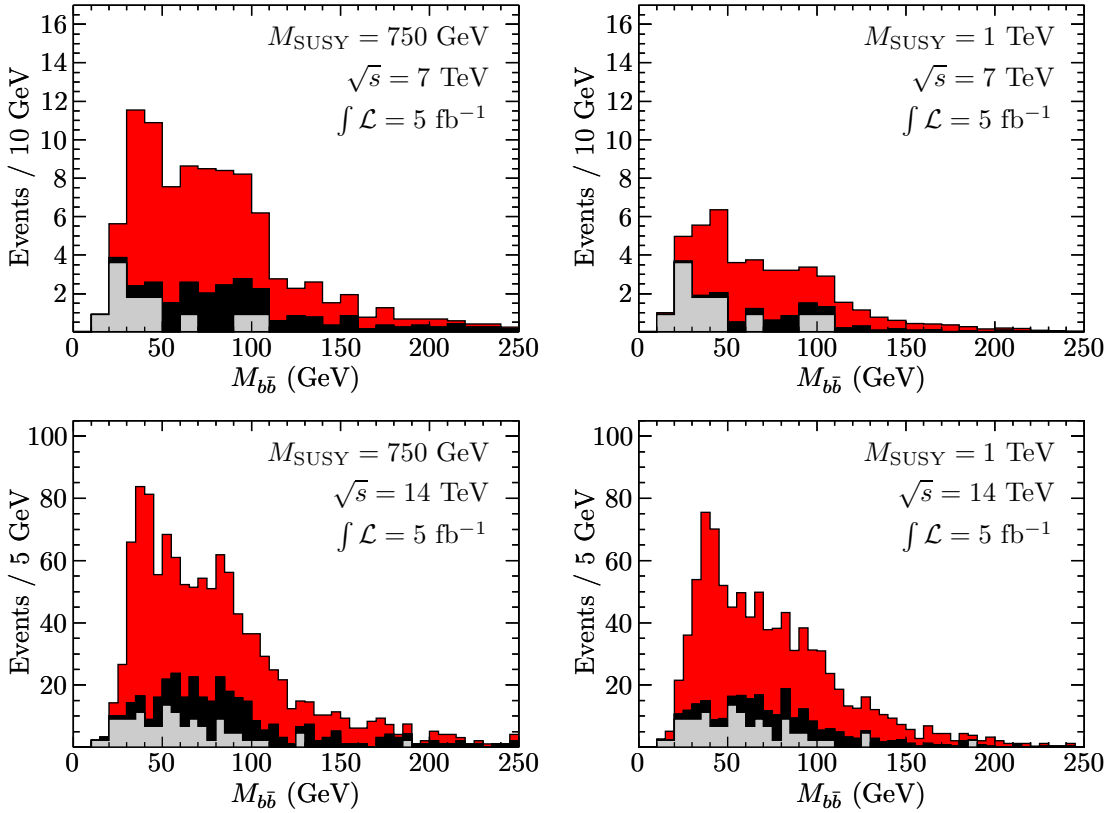

Figure 1: Invariant mass of b-jet pairs for SUSY signal (red), SUSY background (black) and SM $t\bar{t}$ background (light gray) in the considered benchmark scenario with $M_{\mathrm{SUSY}} = 750$ GeV (left column) and $M_{\mathrm{SUSY}} = 1$ TeV (right column) at 7 TeV (upper row) and 14 TeV (lower row) for an integrated luminosity of 5 fb^{-1}. Figures taken from Ref. [1].

2.2 Interpreting the LHC Higgs search results in the MSSM

In view of the excess observed at about 125 GeV in the Higgs searches at the LHC in December 2011, in Ref. [3] the implications of a possible Higgs signal were discussed within the context of the minimal supersymmetric Standard Model (MSSM), taking into account previous limits from Higgs searches at LEP, the Tevatron and the LHC. It was pointed out that the observed excess with a mass of about 125 GeV was well compatible with the predictions of the MSSM, while the observation of a SM-like Higgs boson with a mass above about 135 GeV would have unambiguously ruled out the MSSM with TeV-scale SUSY particles (but would have been viable in the SM and in non-minimal supersymmetric extensions of it). Interpreting the observed excess as signal within the MSSM, the consequences for the remaining MSSM parameter space were investigated. Under the assumption of a Higgs signal new lower bounds on the tree-level parameters of the MSSM Higgs sector were derived. Both the possibilities of associating the observed excess with the light CP-even Higgs boson of the MSSM, h, and the the heavier CP-even Higgs boson H, were investigated. It was demonstrated that also the somewhat exotic

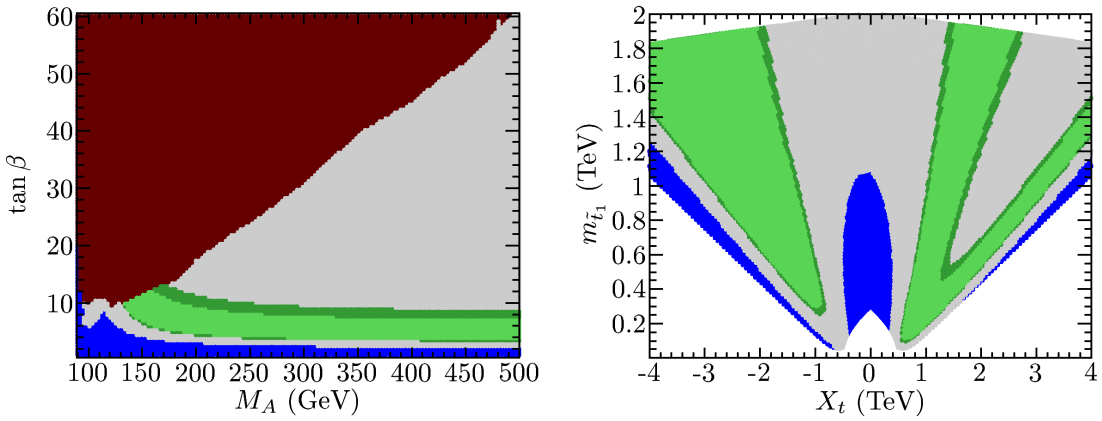

Figure 2: Left: Tree-level Higgs sector parameters (M_A, $\tan\beta$) for the case where the parameters governing the higher-order corrections are chosen such that a maximum value for M_h is obtained ($m_h^{\max}$ benchmark scenario). The different colours correspond to the regions excluded by LEP (blue) and Tevatron/LHC (red). The gray area is the allowed parameter space prior to the observation of an excess at the LHC. The green band shows the region where M_h is compatible with the observed excess. Right: Constraints on the MSSM stop sector from the assumed Higgs signal. The allowed ranges are shown in the (X_t, $M_{\rm SUSY}$) plane (left) and the (X_t, $m_{\tilde{t}_1}$) plane (right) for $M_A = 1$ TeV, $\tan\beta = 20$. The colour coding is as in the left plot. Figures taken from Ref. [3].

possibility that the observed excess was in fact caused by the heavier CP-even Higgs boson (while the lighter one escaped the search limits) was compatible with the data.

Results for the interpretation of the observed excess in terms of the light CP-even Higgs boson of the MSSM are displayed in Fig. 2, showing that there is a significant parameter space of the MSSM compatible with this interpretation. In the left plot of Fig. 2 the parameters that enter via the (in general) numerically large higher-order corrections in the MSSM Higgs sector were set to their values in the $m_h^{\max}$ benchmark scenario, which maximizes the upward shift in M_h as compared to the tree-level value. In this way conservative lower limits on the parameters governing the M_h prediction at tree level, M_A and $\tan\beta$, could be obtained. Taking into account conservatively estimated theoretical uncertainties from unknown higher orders as well as the most important parametric uncertainties arising from the experimental error on the top-quark mass, compatibility with the observed excess yields the lower bounds $M_A > 133$ GeV and $\tan\beta > 3.2$ (for $M_{\rm SUSY} = 1$ TeV). The bound on M_A translates directly into a lower limit $M_{H^\pm} > 155$ GeV, which restricts the kinematic window for MSSM charged Higgs production in the decay of top quarks.

The approach followed in the right plot of Fig. 2 was to choose values for M_A and $\tan\beta$ in the decoupling region and to investigate the constraints on the scalar top and bottom sector of the MSSM from the required compatibility with the observed excess. It was found that a lightest stop mass as light as $m_{\tilde{t}_1} \sim 100$ GeV was still compatible with the observed excess. The bound on $m_{\tilde{t}_1}$ raises to $m_{\tilde{t}_1} \gtrsim 250$ GeV if one restricts to the negative sign of the stop mixing parameter $X_t \equiv A_t - \mu/\tan\beta$, which in general yields better compatibility with the constraints from BR($b \to s\gamma$).

Concerning the interpretation of the observed excess in terms of the heavier CP-even Higgs boson, a scan over M_A, $\tan\beta$, $M_{\rm SUSY}$ and X_t was performed, yielding an allowed area at low M_A and moderate $\tan\beta$. A SM-like rate for production and decay of the heavier CP-even Higgs in the relevant search channels at the LHC is possible for large values of μ and large mixing in the stop sector. It is interesting to note that in the scenario where the assumed Higgs signal is interpreted in terms of the heavier CP-even Higgs boson H the mass of the lighter Higgs, M_h, always comes out to be *below* the SM LEP limit of 114.4 GeV (with reduced couplings to gauge bosons so that the limits from the LEP searches for non-SM like Higgs bosons are respected). It was pointed out that the fact that scenarios of this kind are phenomenologicall viable should serve as a strong motivation for extending the LHC Higgs searches, most notably in the $\gamma\gamma$ final states, also to the mass region below 100 GeV.

3 The discovery and properties of the Higgs boson

3.1 The discovery

Simulation studies performed before the start of data taking had estimated that more than $10\,\text{fb}^{-1}$ collected at $\sqrt{s} = 14\,\text{TeV}$ would be needed to reach a discovery significance of $5\,\sigma$ for a Standard Model Higgs boson with a mass of 125 GeV [4]. In fact, with about $4.8\,\text{fb}^{-1}$ collected at $\sqrt{s} = 7\,\text{TeV}$ in 2011 and about $5.8\,\text{fb}^{-1}$ collected at $\sqrt{s} = 8\,\text{TeV}$, the observed (expected) significance for an excess of events near 126 GeV was $4.5\,\sigma$ ($2.5\,\sigma$) in the $H \to \gamma\gamma$ channel and $5.9\,\sigma$ ($4.9\,\sigma$) after combination with the $H \to ZZ^* \to 4\ell$ and $H \to WW^* \to 2\ell 2\nu$ decay channels in the ATLAS experiment [5]. When considering the look-elsewhere-effect, the observed significance was reduced to $5.1\,\sigma$. Very similar results were obtained by the CMS experiment [6], finding an observed (expected) significance of $5.0\,\sigma$ ($5.8\,\sigma$). With these results, the two experiments had discovered a new particle with properties consistent with those expected from a SM Higgs boson.

The analysis in the $H \to \gamma\gamma$ decay channel employed event categorisation, which improved the sensitivity of the analysis by more than 20%. The categorisation was based on the kinematic properties of the photon candidates, on whether or not the photon candidates were reconstructed as converted photons, and on the event topology, defining also two categories with topology as expected from vector boson fusion production. The event categorisation in Fig. 3 shows the weighted invariant mass spectrum at the time of the discovery. The weighting gives a visual representation of the effect of the categorisation on the analysis.

3.2 Property studies of the new particle

After the discovery, the focus turned to studies of the properties of the new particle to determine whether or not they are consistent with the properties expected from the SM. This included studies of the spin and CP properties, as well as measurements of cross sections and branching ratios, which are sensitive to the coupling of the Higgs boson to SM particles.

3.2.1 Search for and discovery of Higgs boson decays to τ leptons

The discovery had been made in Higgs decays to two bosons, and one important outstanding question was whether or not the mass of fermions is generated by Yukawa couplings. One important channel to study the Higgs couplings to fermions is the Higgs boson decay to two

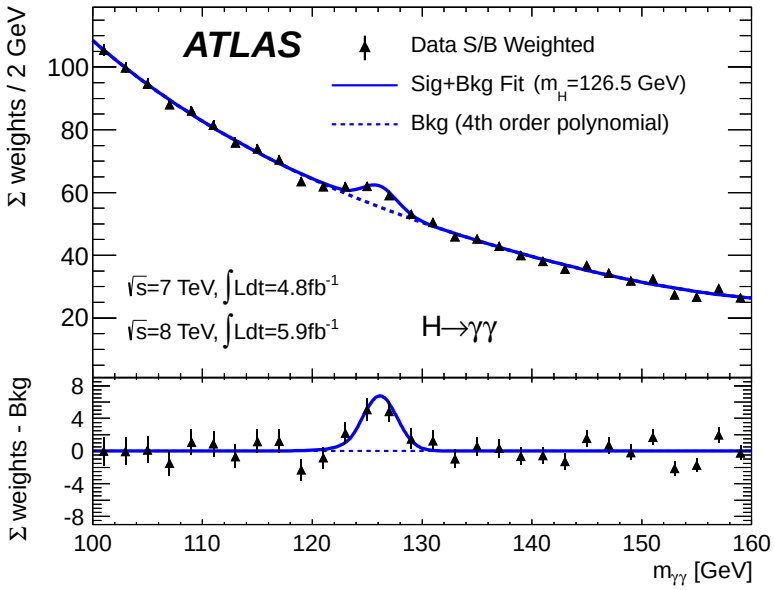

Figure 3: Invariant diphoton mass distribution from the $H \to \gamma\gamma$ discovery analysis. The weight w_i for events in category i is defined to be $\ln(1+S_i/B_i)$, where S_i is 90% of the expected signal for $m_H = 126.5\,\text{GeV}$, and B_i is the integral in the smallest window containing S_i signal events. Figure taken from Ref. [5].

τ leptons. Evidence for the Higgs boson decay to τ leptons was first established with LHC Run 1 data, and the decay was then observed with statistical significance of 5.9 standard deviations after combining Run 1 and Run 2 LHC data collected with the CMS detector [7, 8]. The invariant di-tau mass distribution from the observation of the Higgs decay to τ leptons is shown in Fig. 4.

3.2.2 Simplified template cross sections – development and measurements

In the LHC Run 1, the production processes were measured inclusively, i.e. in the full phase space, and as signal strengths, i.e. as the ratio of the measured and the predicted cross section. It is virtually impossible to update the signal strength measurement of the different Higgs production processes performed in Run 1 when improved theoretical predictions become available. In addition, the interpretation of the measurements would greatly benefit from more differential information. This motivated the discussions and work to develop the Simplified Template Cross Section (STXS) framework in a collaborative effort between theory and experiment [9, 10]. The framework defines kinematic regions for each production process ("bins"), in which the cross section for the given production process will be measured. The definition of the bins is motivated by the goals to reduce the theoretical uncertainties that are folded into the measurement, and to provide measurements useful for reinterpretation, including bins that are particularly sensitive to BSM effects. Different "stages" are defined to allow for measurements with different granularity. In addition, schemes for the parametrisation of the theoretical uncertainties were developed [11].

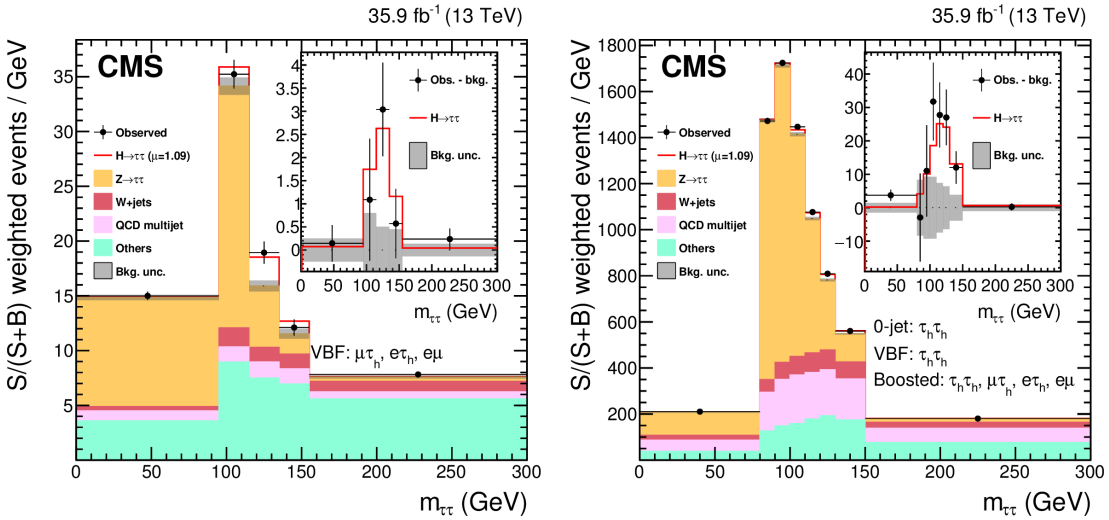

Figure 4: Invariant di-tau mass distribution from the $H \to \tau\tau$ analysis. Figure taken from Ref. [8].

Figure 5 (left) shows "merged stage-1" STXS measurements from $H \to \gamma\gamma$ decays using 80 fb^{-1} collected with the ATLAS detector [12]. The categories defined to target $t\bar{t}H$ production also contributed to the discovery of the $t\bar{t}H$ production process [13]. Figure 5 (right) shows "merged stage-1" STXS measurements obtained from a combination of results obtained in the $H \to \gamma\gamma$ and $H \to 4\ell$ decay channels using 36 fb^{-1} collected with the ATLAS detector [14]. With the dataset collected in Run 2 so far, several bins in jet multiplicity and Higgs boson transverse momentum could be measured for gluon fusion production, as well as bins sensitive to vector boson fusion production.

3.3 Property determinations (theory)

On the theory side, contributions were made to the determination of the spin and CP properties of the detected state [15], to the analysis of off-shell effects [16, 17], and to the determination of Higgs-boson couplings [15, 18, 19].

Concerning the coupling determination, in general a modification of a coupling with respect to the SM prediction may give rise to a change of both the coupling strength and the tensor structure of the coupling, where the latter will affect the CP properties of the coupling. Accordingly, the tasks of determining the couplings and CP properties of the observed signal are in fact closely related to each other. In order to reduce the complexity of the analyses for determining coupling properties during Run 1, an "interim framework" has been introduced in Ref. [18]. It was adopted by the LHC Higgs Cross Section Working Group [19] and used by the ATLAS and CMS collaborations for their experimental analyses. The developed framework consists of a parametrisation of small deviations from SM-like behaviour of the couplings for various benchmark scenarios, based on several simplifying assumptions, in particular: the signals observed in the different search channels are assumed to originate from a single resonance; the width of the observed particle is neglected, so that the predicted rate for a given channel can be decomposed

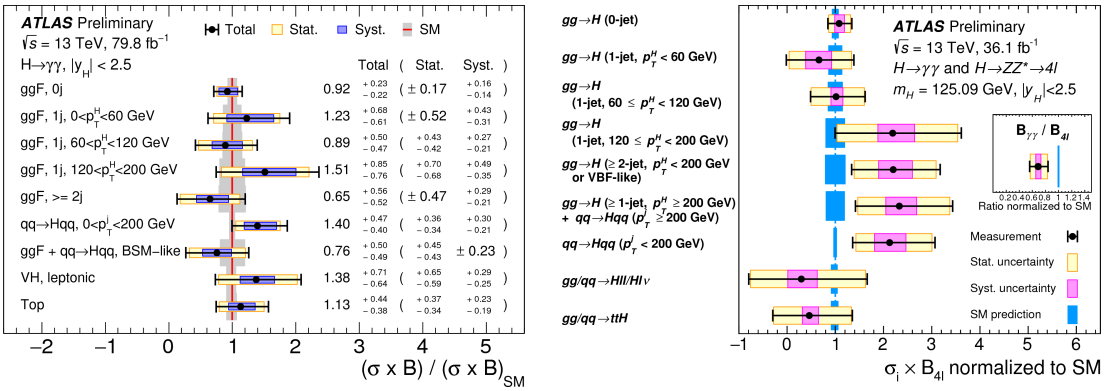

Figure 5: STXS measurements using a "merged stage-1" scheme in the $H \to \gamma\gamma$ decay channel with $80\,\mathrm{fb}^{-1}$ (left), and obtained from combining measurements in $H \to \gamma\gamma$ and $H \to 4\ell$ with $36\,\mathrm{fb}^{-1}$ (right). Figures taken from Refs. [12] and [14], respectively.

into the production and decay contributions, $\sigma \cdot \mathrm{B}(i \to H \to f) = \sigma_i \cdot \Gamma_f / \Gamma_H$, where σ_i is the production cross section through the initial state i, B and Γ_f are the branching ratio and partial decay width into the final state f, respectively, and Γ_H is the total width of the Higgs boson; only modifications of coupling strengths are considered, while the tensor structure of the couplings is assumed to be the same as in the Standard Model – this assumption implies in particular that the observed state is assumed to be a CP-even scalar.

Coupling scale factors κ_j were defined in such a way that the cross sections σ_j and the partial decay widths Γ_j associated with the SM particle j scale with κ_j^2 compared to the SM prediction. By definition, the best available SM predictions for all $\sigma \cdot \mathrm{B}$, including higher-order QCD and electroweak corrections, are recovered when all $\kappa_j = 1$. Since the LHC measurements always involve a combination of Higgs couplings from the production and the decay processes and since there is limited access to the total Higgs-boson width, without further theoretical assumptions only ratios of couplings can be measured at the LHC rather than absolute values of the couplings. The different proposed benchmark scenarios correspond to different assumptions on which of the couplings are fixed to their SM values and for which of them deviations from their SM strengths are considered.

4 Possible interpretations of the detected Higgs signal

4.1 Confronting supersymmetric models with the Higgs signal observed at the LHC

In Ref. [20] the experimental information on the discovered new state was confronted with the predictions in the MSSM and the NMSSM. Performing a scan over the relevant regions of parameter space in both models it was analysed in particular to what extent a significant enhancement of the $\gamma\gamma$ rate of the new particle with respect to the SM prediction could occur in the two models.

Enhancements of this kind are indeed possible in view of limits on the parameter space arising from theoretical constraints as well as from the limits from direct searches for super-

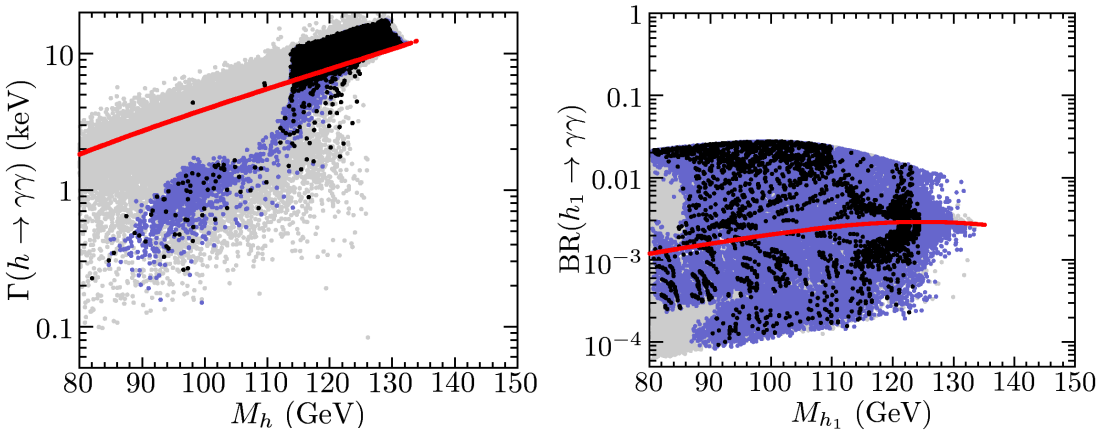

Figure 6: Results from parameter scans in the MSSM (left) and the NMSSM (right) for the decay of the lightest CP-even Higgs boson of the model into a pair of photons. The full result of the scan (all points allowed by the theoretical constraints and the direct search limits for sparticles) is shown in grey. The blue points are compatible with the direct Higgs search limits at that time (from `HiggsBounds 3.6.1`, which included LHC results up to the year 2011), while the black points in addition give a result in agreement with $(g-2)_\mu$ and BR$(b \to s\gamma)$. The left plot shows the partial decay width $\Gamma(h \to \gamma\gamma)$ in the MSSM, while the right plot shows the branching ratio BR$(h_1 \to \gamma\gamma)$ in the NMSSM. The solid (red) curve shows the respective quantities evaluated in the SM. Figures reprinted from Ref. [20] with kind permission of The European Physical Journal (EPJ).

symmetric particles, from the Higgs searches at LEP, the Tevatron and the LHC (incorporating the limits known at that time), from electroweak precision observables and from flavour physics, as can be seen in Fig. 6. Mechanisms that can lead to an enhanced $\gamma\gamma$ rate in comparison to the SM prediction have been analysed in the two models. Within the MSSM, besides the presence of light scalar taus, in particular a suppression of the $b\bar{b}$ decay mode results in an enhanced $\gamma\gamma$ rate. This suppression can either be caused by Higgs-boson propagator corrections entering the effective mixing angle, or by non-decoupling SUSY corrections affecting the relation between the bottom quark mass and the bottom Yukawa coupling. Within the NMSSM the same mechanisms as in the MSSM can be realised. In addition, there exist mechanisms that are genuine for the NMSSM. It was pointed out that in particular the doublet-singlet mixing can result in a substantial suppression of the $b\bar{b}$ mode and an associated enhancement of the $\gamma\gamma$ rate.

The possible interpretation of the discovered Higgs signal in terms of either the light or the heavy CP-even Higgs boson of the MSSM has been investigated in detail in Refs. [21,22]. MSSM fits have been performed of the various rates of cross section times branching ratio as measured by the LHC and Tevatron experiments under the hypotheses of either the light or the heavy CP-even Higgs boson being the new state around 125 GeV, with and without the inclusion of further low-energy observables. An overall good quality of the fits has been found, in the case of the interpretation in terms of the light CP-even Higgs even slightly better than for the SM [21]. Besides the decoupling limit, also the possibility of alignment without decoupling has been investigated. It has furthermore been demonstrated that also the heavy CP-even Higgs

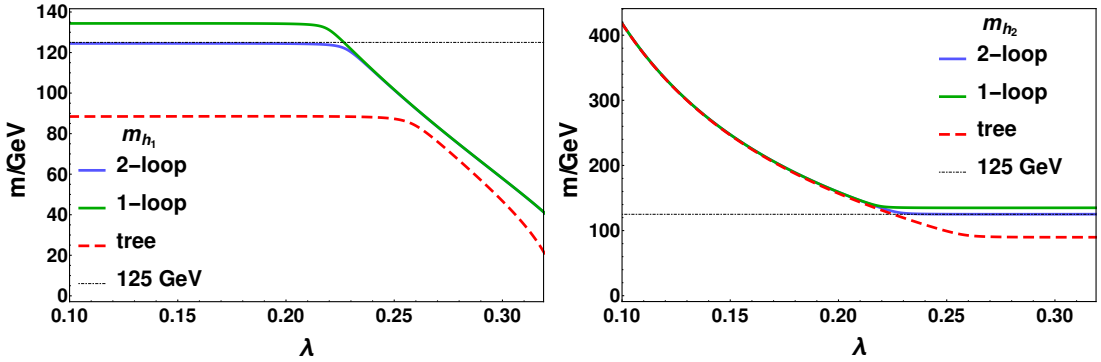

Figure 7: Mass predictions for the lightest and next-to lightest CP-even Higgs-states, m_{h_1} (left), and m_{h_2} (right), of the NMSSM at tree-level, one-loop and two-loop order. Figures taken from Ref. [23].

boson continues to be a viable candidate to explain the Higgs signal – albeit only in a highly constrained parameter region, which is probed by LHC searches for the CP-odd Higgs boson and the charged Higgs boson. The SUSY fits have been carried out in close cooperation with the B8 project of the SFB 676 on global fits.

While as explained above the case where the signal at 125 GeV is not the lightest Higgs boson in the spectrum is tightly constrained in the MSSM, it is important to notice that such a scenario is a quite typical feature of many other extensions of the SM. For instance, in the NMSSM an additional light Higgs boson arises generically if the mass scale of the singlet is lower than the one of the doublets. Such a light Higgs boson is only very weakly constrained by present experimental bounds. In Ref. [23] precise predictions for Higgs-boson masses of the NMSSM were obtained. Figure 7 shows predictions for the masses of the lightest and next-to lightest CP-even Higgs-states at tree-level, one-loop and two-loop order as a function of the NMSSM parameter λ. One can see that the variation of λ gives rise to a "cross-over" behaviour between the doublet-like and the singlet-like Higgs state.

Figure 8 shows results of a parameter scan in the NMSSM for the two lightest neutral Higgs bosons [24]. The state at 125 GeV in Fig. 8 has a small singlet component and can be identified with the Higgs signal observed at the LHC. The model predicts an additional lighter Higgs boson, which has a mass of about 105 GeV in this case, with a large singlet component giving rise to suppressed couplings to the gauge bosons and fermions of the SM. The coloured regions with the indicated best-fit points are in agreement with the experimental results on the Higgs signal and with the limits from Higgs searches as implemented in the public tools `HiggsSignals` [21, 25, 26] and `HiggsBounds` [27, 28].

4.2 Benchmark scenarios for MSSM Higgs searches after the discovery of a Higgs-like particle

In view of the discovered signal new low-energy benchmark scenarios have been proposed for MSSM Higgs searches in Ref. [29]. Those benchmarks are over a wide parameter range compatible with the mass and production rates of the observed signal. The proposed scenarios also exhibit interesting phenomenology for the MSSM Higgs sector. They comprise in particular a

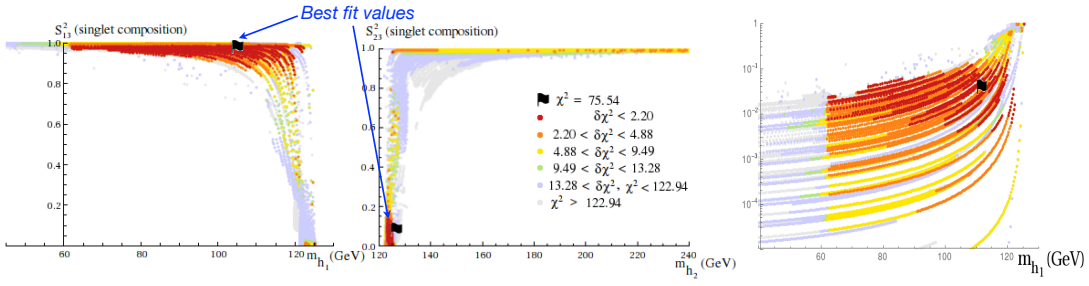

Figure 8: Results of a parameter scan in the NMSSM for the two lightest neutral Higgs bosons. The regions that are preferred by the fit in the vicinity of the indicated best points are shown in red. The plots show the singlet composition of the lightest two states (left) and the squared coupling of the lightest Higgs state to gauge bosons, normalised to the SM value. Figures taken from Ref. [24].

slightly modified version of the well-known $m_h^{\rm max}$ scenario, called $m_h^{\rm mod}$, where the light CP-even Higgs boson can be interpreted as the LHC signal in large parts of the M_A–$\tan\beta$ plane, see Fig. 9. Furthermore, a light stop scenario leading to a suppression of the lightest CP-even Higgs gluon fusion rate, a light stau scenario with an enhanced decay rate of h to $\gamma\gamma$ at large $\tan\beta$, and a τ-phobic Higgs scenario in which the lightest Higgs boson can have suppressed couplings to down-type fermions have been defined. The importance of investigating different values of both signs of the parameter μ has been emphasized. For the default value of $\mu = 200$ GeV sizeable branching ratios of the heavy Higgs bosons into charginos and neutralinos occur, see Fig. 9. In addition to the scenarios where the lightest CP-even Higgs boson is interpreted as the LHC signal, also a low–M_H scenario has been proposed, where instead the heavy CP-even Higgs boson corresponds to the new state around 125 GeV (see above). See Ref. [30] for a recent update of the MSSM benchmark scenarios.

5 Precise predictions for Higgs physics in supersymmetric models

A particular effort in the research activities has been devoted to precise predictions for Higgs physics in supersymmetric models. In this context in particular the public code `FeynHiggs`[†] [31–37] has been further developed, including an ongoing effort of extending the predictions from the MSSM to the NMSSM [23, 38, 39]. In the following only a few examples of the accomplished results will be mentioned.

5.1 Improved two-loop predictions in the MSSM with complex parameters

In Refs. [40] and [41] improved two-loop results for the Higgs-boson masses of the MSSM have been obtained for the general case of arbitrary complex parameters. The corresponding self-energies and their renormalization have been obtained in the Feynman-diagrammatic approach.

[†] see `www.feynhiggs.de`

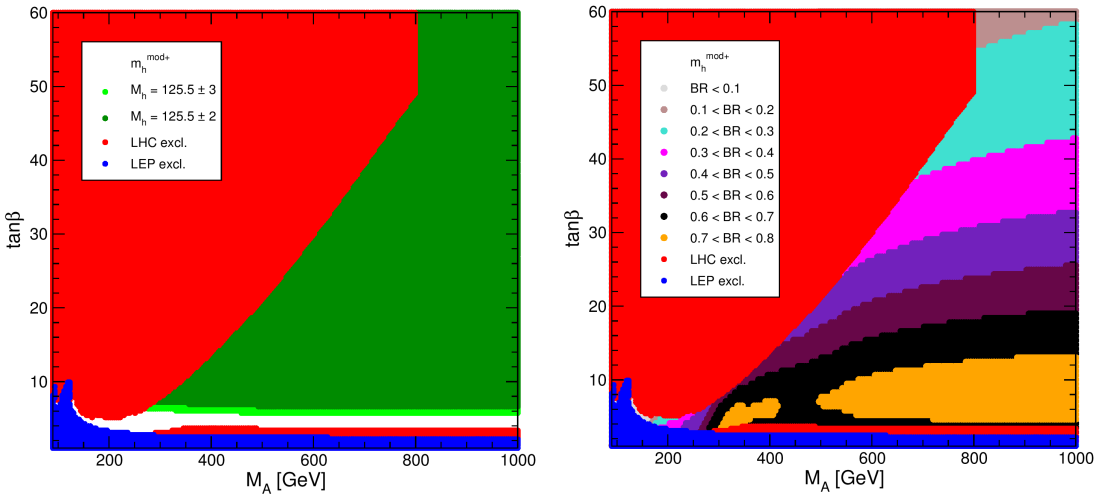

Figure 9: The M_A–$\tan\beta$ plane in the $m_h^{\mathrm{mod+}}$ scenario. The excluded regions from LEP and the LHC as obtained from `HiggsBounds` [27,28] at the time of writing [29] are indicated in blue and red, respectively. In the left plot the favoured region $M_h = 125.5 \pm 2(3)$ GeV is shown in green, while in the right plot the colour coding in the allowed region indicates the average total branching ratio of H and A into charginos and neutralinos. Figures reprinted from Ref. [29] with kind permission of The European Physical Journal (EPJ).

In Ref. [40] the corrections of $\mathcal{O}\left(\alpha_{\mathrm{t}}^2 + \alpha_{\mathrm{t}}\alpha_{\mathrm{b}} + \alpha_{\mathrm{b}}^2\right)$ from the Yukawa sector in the gauge-less limit have been calculated, while in Ref. [41] the complete two-loop QCD contributions to the mass of the lightest Higgs boson in the MSSM have been obtained.

In the result of Ref. [41] the full dependence on the external momentum and all relevant mass scales has been taken into account at the two-loop level without any approximation. The evaluation of the involved two-loop two-point integrals with up to five different mass scales was carried out with numerical methods. The impact of the new contributions on the Higgs spectrum can be seen in Fig. 10. In the left plot the prediction for M_{h_1} as a function of $\tan\beta$ is compared in an $m_h^{\mathrm{mod+}}$-like scenario with the previous result including and excluding the $\mathcal{O}\left(\alpha_{\mathrm{b}}\alpha_{\mathrm{s}}\right)$ terms that are known in the MSSM with real parameters. While the effect of the latter is small, the formally sub-leading two-loop contributions in our new result yield an upward shift of about 0.85 GeV compared to the previous result over a wide range of $\tan\beta$ values. In the right plot the prediction for M_{h_1} is shown as function of the gluino phase ϕ_{M_3}. The plot shows a sensitive dependence on the gluino phase, which enters at the two-loop level, and again a sizeable upward shift of the new result as compared to the previous result.

5.2 Combination of fixed-order results and effective field theory methods for precise Higgs-mass predictions

The precisely measured experimental value of the detected Higgs state can be confronted with models like supersymmetric extensions of the Standard Model where the mass of the state that is identified with the observed signal can be predicted from the other model parameters. This

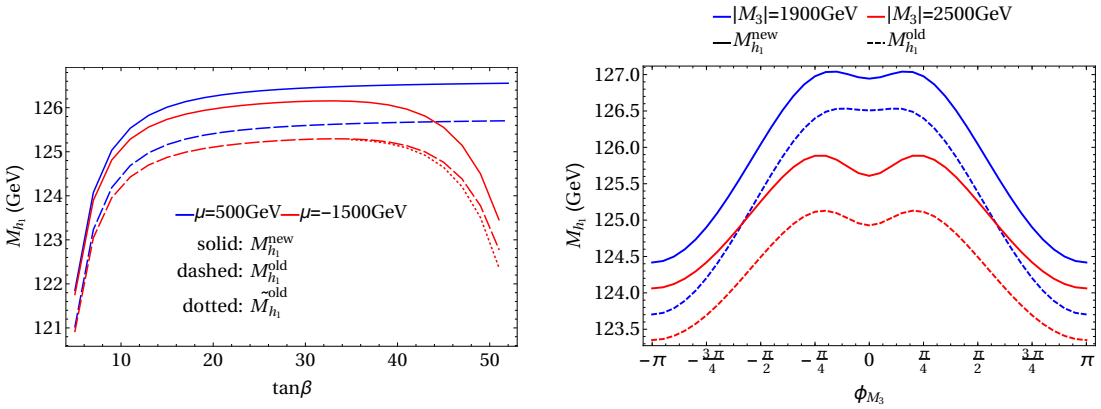

Figure 10: Prediction for the light Higgs-boson mass M_{h_1} as a function of $\tan\beta$ (left) and as a function of the gluino phase ϕ_{M_3} (right). In the left plot the new result (solid) is compared with the previous result (dashed) in an $m_h^{\rm mod+}$-like scenario for two values of μ. The dotted line shows the case where the previous result is supplemented with the $\mathcal{O}(\alpha_{\rm b}\alpha_{\rm s})$ terms that are known in the MSSM with real parameters. In the right plot the new result (solid) is compared with the previous result (dashed) in a scenario with $\tan\beta = 50$ for two values of $|M_3|$. Figures taken from Ref. [41].

confrontation of the experimental value with the model prediction yields sensitive constraints on the parameter space of each model and plays a crucial role in the quest to discriminate between different models. A very high precision of the theoretical predictions is required in order to exploit the high accuracy of the measured mass value. The relatively high value of about 125 GeV of the detected Higgs signal together with the existing limits from direct searches for SUSY particles has led to various investigations where some or all of the SUSY particles are in the multi-TeV range or above. In case of large hierarchies between the electroweak and the SUSY scale a resummation of large logarithmic contributions via effective field theory (EFT) methods is necessary in order to obtain accurate theoretical predictions.

In Ref. [35] a "hybrid approach" improving the prediction for the SM-like state in the MSSM has been developed. It combines the fixed-order result, comprising the full one-loop and leading and subleading two-loop corrections, with a resummation of the leading and subleading logarithmic contributions from the scalar top sector to all orders obtained from solving the two-loop renormalisation group equations. Particular care was taken in this context to consistently match these two different types of corrections. In this way for the first time a high-precision prediction for the mass of the light CP-even Higgs boson in the MSSM was obtained that is valid from the electroweak scale up to the multi-TeV region of the relevant supersymmetric particles. The results were implemented into the public code `FeynHiggs`. In Fig. 11 the pure fixed-order result as a function of the SUSY scale, for two values of the parameter X_t controlling the mixing in the scalar top sector, is compared with the result including the resummation of leading and next-to-leading logarithmic contributions to all orders. Furthermore, the results of an analytic solution of the renormalisation group equations at the 3-loop to 7-loop level are also shown. While the impact of the higher-order logarithmic contributions is relatively small for SUSY scales around 1 TeV, they give rise to large effects for higher values of M_S.

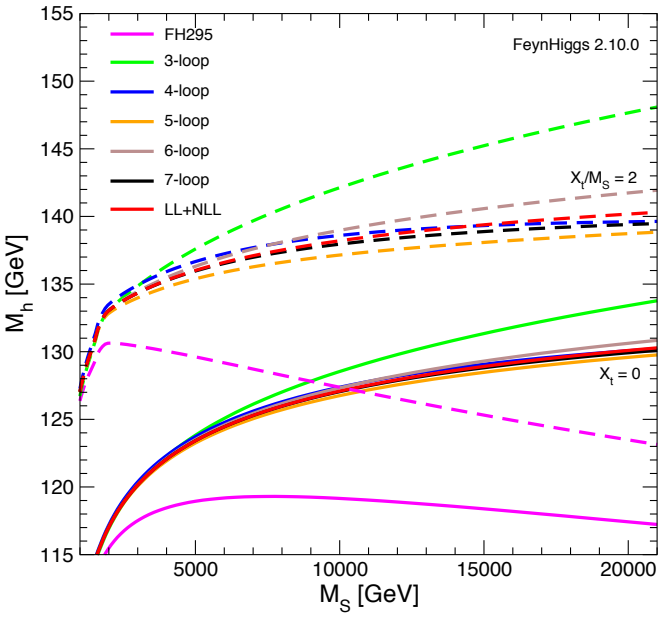

Figure 11: Prediction for the light Higgs-boson mass M_h as a function of the SUSY scale M_S for $X_t = 0$ (solid) and $X_t/M_S = 2$ (dashed). The full result including a resummation of logarithmic contributions ("LL+NLL") is compared with results containing the logarithmic contributions up to the 3-loop, ..., 7-loop level and with the previous fixed-order result ("FH295"). Reprinted figure with permission from Ref. [35]. Copyright (2014) by the American Physical Society.

The predictions obtained in the hybrid approach have been further improved by including the full next-to-leading-logarithmic (NLL) and a partial next-to-NLL (NNLL) resummation of the large logarithmic corrections. In Ref. [37] a detailed analytical comparison of the hybrid approach and the pure EFT approach has been carried out, and the numerical results of `FeynHiggs` have been confronted with the ones of the EFT code `SUSYHD` [42]. The sources of several discrepancies that were previously reported in the literature could be resolved, and the remaining deviations were discussed.

6 Searches for rare and non-SM decays of the detected Higgs boson and for non-SM Higgs bosons

6.1 Search for decays to two muons

The simple relation

$$g_{Hff} = \sqrt{2}\frac{m_f}{v}$$

between the mass m_f of a fermion, the Higgs–fermion coupling g_{Hff}, and the vacuum expectation value v is one of the central assumptions of the Standard Model. Experimentally however, this could be tested up to now only for the heavy fermions of the third generation. Since the

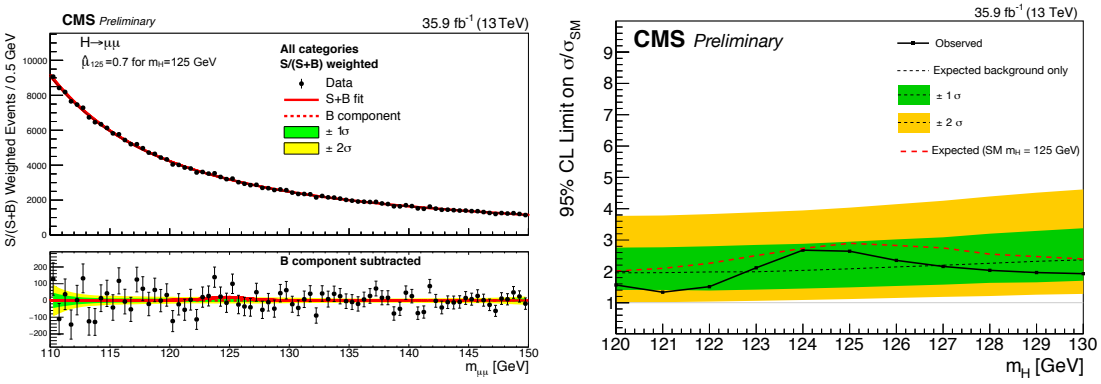

Figure 12: Left: Weighted distribution of measured invariant masses of $\mu^+\mu^-$ pairs in comparison to the sum of fits of signal and background to all event categories. Right: Limit on the cross section in relation to the Standard Model prediction. Figures taken from Ref. [43].

branching ratios $H \to f\bar{f}$ depend on g^2_{Hff} the only hope to probe this prediction for the other generations are $H \to c\bar{c}$ decays, where however the background from other processes is vast, and $H \to \mu^+\mu^-$ decays. For the latter case the background consists mostly of Drell-Yan events with off-shell Z/γ and of leptonic decays of W^+W^-- and $t\bar{t}$-pairs. This background is way lower than for the $c\bar{c}$ case, but due to the expected small branching ratio $\mathrm{B}(H \to \mu^+\mu^-) = 2.18 \times 10^{-4}$ still much larger than the signal process. For a search conducted by the CMS collaboration [43] the excellent invariant mass resolution of the $\mu^+\mu^-$ pair is employed. Using observables uncorrelated to $m_{\mu^+\mu^-}$ a boosted decision tree is used to classify events according to the Higgs production topology. The resulting weighted event disctribution is shown in Fig. 12. In combination with previous data obtained at lower centre of mass energy this search leads to an observed (expected) limit on the cross section times branching ratio, which is a factor 2.92 (2.16) larger than the Standard Model prediction.

A future aim of this analysis is to measure for the first time a Higgs coupling to second generation fermions by including data from 2017 and 2018.

6.2 Search for lepton-flavour violating decays

In many extensions of the Standard Model and in particular in classes of two-Higgs doublet models the fermion–Higgs couplings do not have to be flavour diagonal but allow for lepton flavour violating decays such as $H \to \tau^\pm\mu^\mp$, $H \to \tau^\pm e^\mp$, $H \to \mu^\pm e^\mp$ (cf. references in Ref. [44]). The emerging final states have a striking signature at the LHC with low Standard Model background, so that sensitivities to the corresponding couplings can be reached which are much stricter than those obtained from searches for rare or forbidden decays such as $\tau \to \mu\gamma$, etc. In an early search for the most promising decay $H \to \tau^\pm\mu^\mp$ using 7 TeV data from CMS, a small excess was observed [45]. This triggered much theoretical work but also searches for the other decay modes using much larger data sets at higher centre of mass energies [44, 46].

In Fig. 13 the event distributions of the most recent data are shown in comparison to various background sources and for a Higgs at a mass of 125 GeV with a branching ratio of 10% into $\tau^\pm\mu^\mp$. As the data for this larger sample agree with the background only expectation, an upper

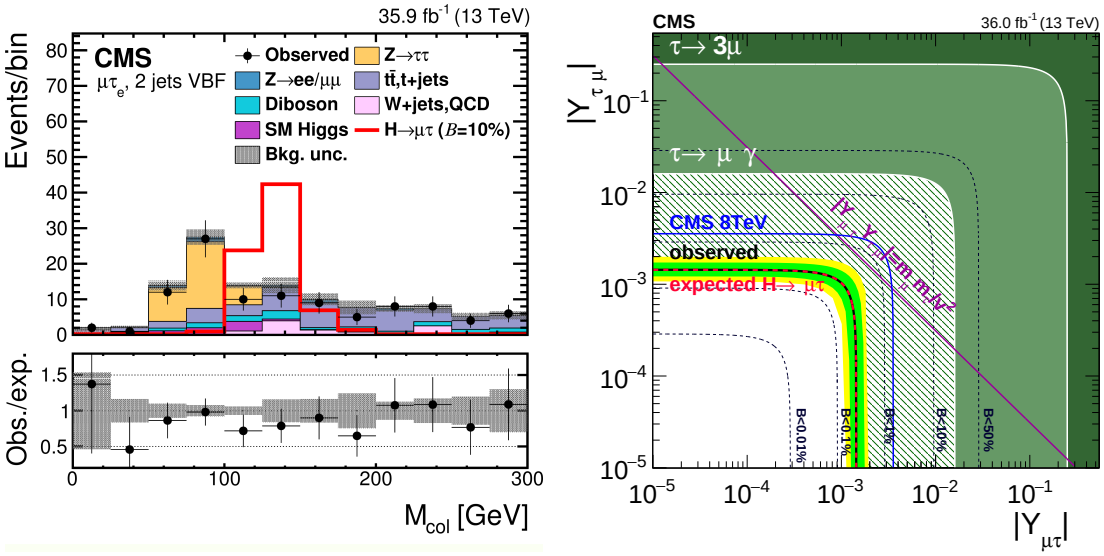

Figure 13: Left: Measured distribution of collinear masses for $H \to \tau^{\pm}\mu^{\mp}$ with the τ decaying into an electron and neutrinos and two further jets to tag vector boson fusion processes. The expected rate for $H \to \tau^{\pm}\mu^{\mp}$ is shown for a branching ratio of 10%. Close to the Higgs mass the background is dominated by $t\bar{t}$ production. Right: Combining analysis for different Higgs production and τ decay modes the limit on the Higgs branching ratio is converted into a limit on the Higgs couplings in the mixing matrix, $Y_{\mu\tau}$ and $Y_{\tau\mu}$. The observed limit is about one order of magnitude stronger than the one from indirect constraints ($\tau \to \mu\gamma$). Figures taken from Ref. [44].

limit on the branching ratio of $\mathrm{B}(H \to \tau^{\pm}\mu^{\mp}) \geq 0.25\%$ was derived.

6.3 Search for decays to $Z\gamma$

In the SM, the Higgs boson decay to $Z\gamma$ proceeds through a loop process, similar to the $H \to \gamma\gamma$ decay. As such, it is sensitive to contributions from physics beyond the SM that could contribute to the loop. In the SM, the branching ratio for the $Z\gamma$ decay is predicted to be $(1.54 \pm 0.09) \times 10^{-3}$, comparable to that for the decay into two photons, but the number of reconstructed events is significantly reduced by considering Z boson decays into electrons or muons, to benefit from a good invariant mass resolution. The search with the data collected in 2015 and 2016 by the ATLAS experiment set an upper limit on $\sigma(pp \to H) \cdot \mathrm{B}(H \to Z\gamma)$ of 6.6 times the SM prediction at the 95% confidence level (CL) [47], corresponding to an upper limit on the branching ratio of Higgs boson decays to $Z\gamma$ of 1% when assuming SM Higgs boson production. The expected 95% CL limit on $\sigma(pp \to H) \cdot \mathrm{B}(H \to Z\gamma)$ assuming SM Higgs boson decay to $Z\gamma$ was 5.2 times the SM prediction.

A future extension of this analysis is a search for the Higgs boson decays into $\gamma^*\gamma$, which is an experimentally more challenging signature since the two leptons have an invariant mass different from the Z-boson mass.

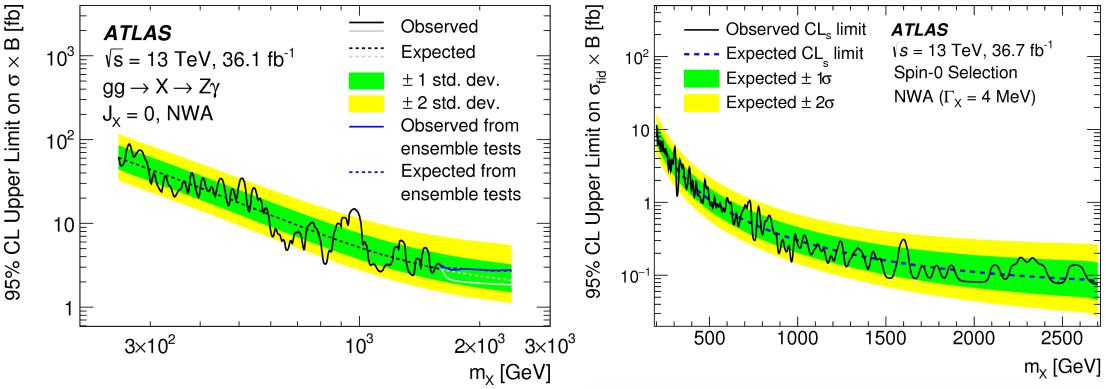

Figure 14: Limits on the cross section times branching ratio for heavy spin-0 particles decaying into $Z\gamma$ (left) or $\gamma\gamma$ (right). Figures taken from Refs. [47] and [48], respectively.

6.4 Search for heavy Higgs bosons decaying to $Z\gamma$ or $\gamma\gamma$

Many extensions of the SM introduce new heavy bosons, for example as extensions of the Higgs sector. Searching for these potential new heavy bosons in decays to $Z(\to \ell\ell)\gamma$ or $\gamma\gamma$ profits from the good invariant mass resolution of these final states, as well as moderate backgrounds. Figure 14 shows the exclusion limits on the cross section times branching ratio for the production of heavy spin-0 particles decaying into $Z\gamma$ or $\gamma\gamma$ at the 95% CL from the analyses performed with the 2015+2016 dataset collected by the ATLAS experiment [47, 48].

Should a new heavy resonance be found at the LHC, one of the first questions to answer would be whether it is produced in gluon or quark initial states. Good sensitivity to identify the initial state can be achieved in a model-independent way by using a tight veto on hadronic jets produced in association with a heavy resonance to divide the data into two mutually exclusive samples, with and without hadronic jets [49], as can be seen in Fig. 15.

6.5 Search for further supersymmetric Higgs bosons

Additional Higgs particles are predicted for example by Two-Higgs-Doublet-Models such as the Minimal Supersymmetric Standard Model (MSSM). Experimental searches for decays of such Higgs particles into Standard Model particles are carried out in a variety of final states. Their relative importance depends of course on the fundamental parameters of the underlying theory.

For heavy neutral Higgs particles (H) in the range $250 \leq M_H \leq 350$ GeV, i.e. above twice the mass of the discovered Higgs boson (h with $m_h = 125$ GeV) and below twice the mass of the top-quark, decays $H \to hh$ often have a large branching ratio. The subsequent final state with one h decaying into $h \to bb$ and the other into $h \to \tau\tau$ has the advantage of a rather large combined branching ratio and well detectable b-quarks and τ-leptons. Furthermore this final state is kinematically overconstrained once the low mass to momentum ratio of the tau leptons is employed to constrain the direction of the neutrinos in the tau decays. A dedicated kinematic fit was developed which in addition makes use of the known value of m_h and of transverse momentum balance in order to drastically improve the resolution for m_H [50]. The analysis of the CMS data using this method actually was able to basically exclude heavy Higgs particles in the MSSM in the stated mass range [51] for low $\tan\beta$.

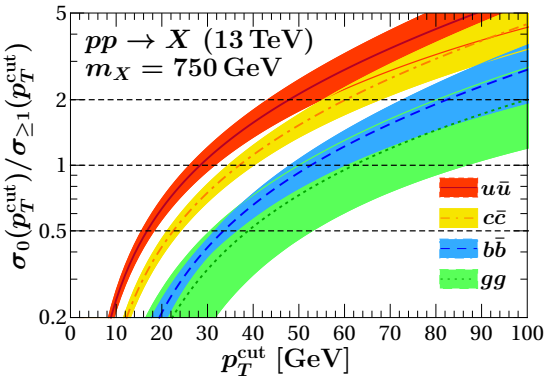

Figure 15: Ratio of the cross section of events produced without hadronic jets to the cross section for events with at least one hadronic jet for different initial states. Reprinted figure with permission from Ref. [49]. Copyright (2016) by the American Physical Society.

Of particular interest are also decay modes of neutral heavy Higgs bosons into pairs of tau leptons. The background estimation techniques and analysis tools developed in the course of the aformentioned studies of the discovered Higgs boson are applicable here as well. Searches performed at different centre of mass energies [52, 53] revealed no signal, and results of the analyses have been used to set upper limits on the Higgs boson production cross section times branching ratio $\mathrm{B}(H \to \tau\tau)$ as well as to put stringent constraints on the model parameters. Within several MSSM benchmark scenarios, results of the search have been translated into exclusion contours in the $(M_A, \tan\beta)$ plane. Typically, values of $\tan\beta$ above 60 are excluded for $M_A > 1.7$ TeV in scenarios where the lightest scalar boson is compatible with the measured properties of the discovered 125 GeV Higgs boson. Figure 16 shows the example of the $m_h^{\rm mod+}$ benchmark scenario [29], see Sec. 4.2. A crucial ingredient to these measurements is the understanding of the τ identification and momentum scale for hadronically decaying τ leptons in the kinematic phase space not accessible via the $Z \to \tau\tau$ standard candle. Their measurement has been done for τ leptons with transverse momentum exceeding 100 GeV in the sample of highly virtually W bosons decaying into τ lepton and neutrino [54].

Searches for heavy neutral supersymmetric Higgs bosons dacaying into b-quarks have also been performed. Since the inclusive search for this signature has low sensitivity because of overwhelming QCD multijet background, Higgs boson production in association with further b-quarks was investigated. This production mode is characterised by an enhanced rate at large values of $\tan\beta$. The analysis has been facilitated by specialized multijet triggers. No signal was found in the searches performed [55, 56]. The results are thus interpreted in a model-independent way by placing upper limits on the product of signal production cross section and branching ratio of decays into b-quarks on $\tan\beta$ as a function of M_A within several MSSM benchmark scenarios. The study has yielded the best world sensitivity to date to the MSSM Higgs bosons in the $H \to bb$ decay mode.

In the Next-to-Minimal Supersymmetric Standard Model (NMSSM) a further singlet is assumed to solve the μ problem. In particular there are scenarios in which a light scalar boson with $M_h < M_Z$ has a large singlet component so that its couplings to the SM particles are suppressed. Therefore conventional present and past searches targeting either gluon-gluon

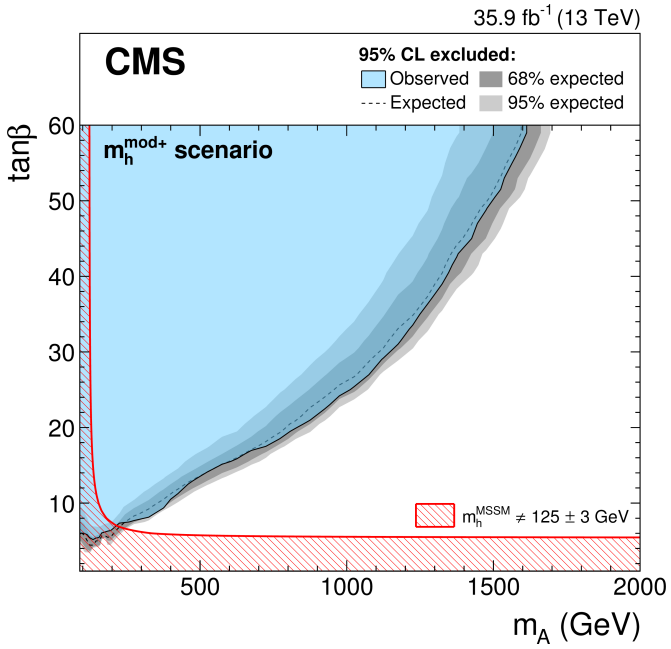

Figure 16: Exclusion bounds from CMS searches for heavy Higgs bosons decaying into a pair of tau leptons in the $(M_A, \tan\beta)$ plane of the MSSM for the $m_h^{\text{mod+}}$ benchmark scenario [29]. Figure taken from Ref. [53].

fusion or b-quark associated production at hadron colliders or Higgs-strahlug process at electron-positron colliders, could miss such a state. Instead it was suggested to search for this light state in cascade decays of coloured SUSY particles [1]. Experimentally the signal was searched for in multijet final state with two b-quarks resulting from the decay of the searched light scalar boson, and therefore exhibiting resonance structure in its invariant mass distribution. No signal was found, and results of the analysis were translated into constraints on the NMSSM parameters. The results of these studies have been presented in Ref. [2].

Also a search for a very light pseudoscalar Higgs boson produced in decays of the 125 GeV boson and decaying into tau lepton pairs was performed. The study probed masses of the pseudoscalar boson in the range $4 \leq m_a \leq 8$ GeV, where the decay of a into a pair of tau leptons dominates at high values of $\tan\beta$. No evidence for a signal has been established, and upper limits on the 125 GeV Higgs boson production cross section times branching ratio of the searched decay, $\text{B}(H \to aa \to 4\tau)$, have been devised as a function of m_a [57].

6.6 Impact of interference effects in the search for additional Higgs bosons

As shown in Ref. [58], interference and mixing effects between neutral Higgs bosons in the MSSM with complex parameters can have a significant impact on the interpretation of LHC searches for additional supersymmetric Higgs bosons. Complex MSSM parameters introduce mixing between the CP-even and CP-odd Higgs states h, H, A into the mass eigenstates h_1, h_2, h_3

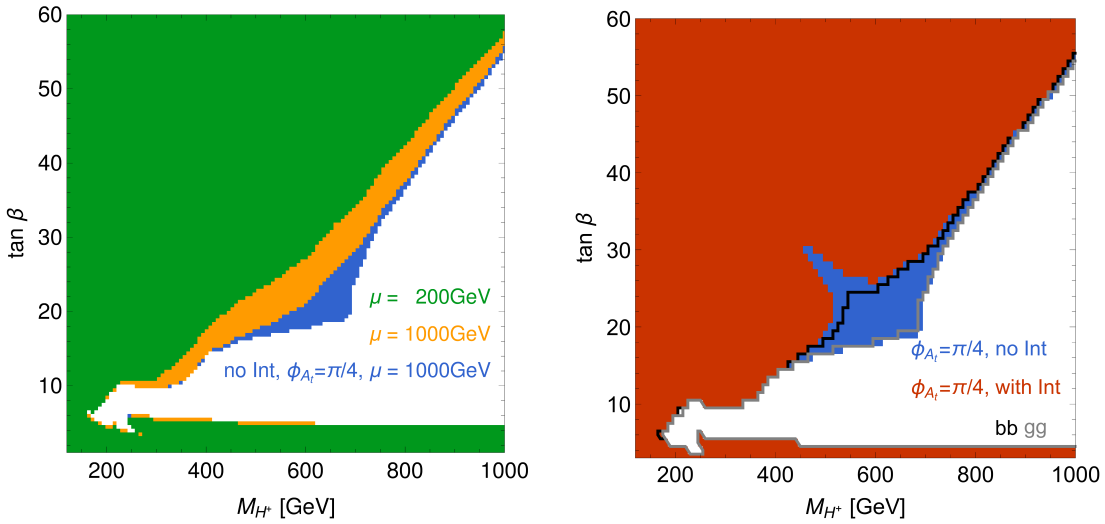

Figure 17: Exclusion bounds in the $(M_{H^\pm}, \tan\beta)$ plane of the MSSM obtained with `HiggsBounds` [27,28]. The left plot shows the results for the $m_h^{\text{mod+}}$ benchmark scenario [29] with real parameters for $\mu = 200$ GeV (green) and $\mu = 1$ TeV (orange) as well as the exclusion bound that would be obtained in the corresponding scenario with $\phi_{A_t} = \pi/4$ and $\mu = 1$ TeV for the incoherent sum of cross sections with 3×3 mixing but without the interference contribution (blue). The blue area is the same in the right plot, where it is compared with the result taking into account the interference contribution in both the $b\bar{b}$ and the gg processes (red). For illustration also the cases where the interference contribution is included only in the $b\bar{b}$ (black line) and only in the gg (grey line) process are shown. Figures taken from Ref. [58].

and generate CP-violating interference terms. Both effects are enhanced in the case of almost degenerate states. Such a situation is typically realised in an extended Higgs sector with a SM-like Higgs state at about 125 GeV, since in the decoupling limit the additional Higgs bosons tend to be heavy and nearly mass-degenerate.

Employing as an example an extension of the $m_h^{\text{mod+}}$ benchmark scenario [29] by a non-zero phase ϕ_{A_t}, the interference contributions for the production of neutral Higgs bosons in gluon-fusion and in association with b-quarks followed by the decay into a pair of τ-leptons have been obtained in Ref. [58]. While the resonant mixing increases the individual cross sections for the two heavy Higgs bosons h_2 and h_3, strongly destructive interference effects between the contributions involving h_2 and h_3 leave a considerable parameter region unexcluded that would appear to be ruled out if the interference effects were neglected. This is shown in Fig. 17, where the exclusion limits obtained from `HiggsBounds` [27,28] are compared with the result that would be obtained if the interference contributions were neglected. The interference contributions give rise to the unexcluded "fjord" in the right plot of Fig. 17 (red area). The chosen scenario with $\mu = 1$ TeV and $\phi_{A_t} = \pi/4$ is compared with the $m_h^{\text{mod+}}$ benchmark scenario [29] with real parameters for $\mu = 200$ GeV and $\mu = 1$ TeV in the left plot of Fig. 17.

7 Conclusions

In this report we have summarized some of the results that have been obtained in the project B9 of the SFB 676, in which the underlying physics of electroweak symmetry breaking has been probed in a joint effort between experimental activities in ATLAS and CMS and theoretical investigations. The presented results comprise theoretical studies preceding the Higgs boson discovery, experimental contributions to the Higgs boson discovery, the determination of properties of the detected state in close interplay between experiment and theory, precise theory predictions and possible interpretations of the detected Higgs signal, as well as experimental and theoretical aspects of searches for physics beyond the Standard Model in the Higgs sector.

The quest to identify the dynamics that is responsible for the generation of the property of mass of elementary particles is one of the most important goals of current fundamental science. The discovery of a Higgs boson has opened up a new window to the exploration of the mechanism of electroweak symmetry breaking and of the structure of the vacuum. In this project, this unique window has been exploited, and a lot of progress has been made within this vibrant field. Future data on searches and precision measurements that can be obtained at the LHC and beyond together with corresponding activities on the theory side provide excellent prospects for further breakthroughs in this area of research.

Acknowledgements

We would also like to thank H. Bahl, P. Bechtle, R. Benbrik, N. Berger, S. Borowka, M. Carena, F. Domingo, P. Drechsel, M. Duehrssen-Debling, M. A. Ebert, P. Francavilla, E. Fuchs, L. Galeta, M. Gomez Bock, N. Greiner, H. Haber, T. Hahn, S. Heinemeyer, W. Hollik, S. Liebler, G. Moortgat-Pick, I. Moult, S. Paßehr, S. Patel, H. Rzehak, O. Stål, T. Stefaniak, I. W. Stewart, F. J. Tackmann, C.E.M. Wagner, and L. Zeune for fruitful collaboration on the results presented in this report. We appreciate the collaboration with our colleagues at CERN and other institutes in the ATLAS and CMS experiments. The work presented in this report has been supported in part by the DFG through the SFB 676 "Particles, Strings and the Early Universe".

References

[1] O. Stål and G. Weiglein, *Light NMSSM Higgs bosons in SUSY cascade decays at the LHC*, *JHEP* **01** (2012) 071, [1108.0595].

[2] CMS Collaboration, *Search for a light NMSSM Higgs boson produced in supersymmetric cascades and decaying into a b-quark pair*, Tech. Rep. CMS-PAS-HIG-14-030, CERN, Geneva, 2015.

[3] S. Heinemeyer, O. Stål and G. Weiglein, *Interpreting the LHC Higgs Search Results in the MSSM*, *Phys. Lett.* **B710** (2012) 201–206, [1112.3026].

[4] ATLAS Collaboration, *Expected Performance of the ATLAS Experiment - Detector, Trigger and Physics*, 0901.0512.

[5] ATLAS Collaboration, *Observation of a new particle in the search for the Standard Model Higgs boson with the ATLAS detector at the LHC*, *Phys. Lett.* **B716** (2012) 1–29, [1207.7214].

[6] CMS Collaboration, *Observation of a new boson at a mass of 125 GeV with the CMS experiment at the LHC*, *Phys. Lett.* **B716** (2012) 30–61, [1207.7235].

[7] CMS Collaboration, *Evidence for the 125 GeV Higgs boson decaying to a pair of τ leptons*, *JHEP* **05** (2014) 104, [1401.5041].

[8] CMS Collaboration, *Observation of the Higgs boson decay to a pair of τ leptons with the CMS detector*, *Phys. Lett.* **B779** (2018) 283–316, [1708.00373].

[9] J. R. Andersen et al., *Les Houches 2015: Physics at TeV Colliders Standard Model Working Group Report*, in *9th Les Houches Workshop on Physics at TeV Colliders (PhysTeV 2015) Les Houches, France, June 1-19, 2015*, 2016, 1605.04692, http://lss.fnal.gov/archive/2016/conf/fermilab-conf-16-175-ppd-t.pdf.

[10] LHC Higgs Cross Section Working Group, D. de Florian et al., *Handbook of LHC Higgs Cross Sections: 4. Deciphering the Nature of the Higgs Sector*, 1610.07922. 10.23731/CYRM-2017-002.

[11] J. R. Andersen et al., *Les Houches 2017: Physics at TeV Colliders Standard Model Working Group Report*, in *10th Les Houches Workshop on Physics at TeV Colliders (PhysTeV 2017) Les Houches, France, June 5-23, 2017*, 2018, 1803.07977, http://lss.fnal.gov/archive/2018/conf/fermilab-conf-18-122-cd-t.pdf.

[12] ATLAS Collaboration, *Measurements of Higgs boson properties in the diphoton decay channel using 80 fb^{-1} of pp collision data at $\sqrt{s}$ = 13 TeV with the ATLAS detector*, Tech. Rep. ATLAS-CONF-2018-028, CERN, Geneva, 2018.

[13] ATLAS Collaboration, ATLAS Collaboration, *Observation of Higgs boson production in association with a top quark pair at the LHC with the ATLAS detector*, *Phys. Lett.* **B784** (2018) 173–191, [1806.00425].

[14] ATLAS Collaboration, *Combined measurements of Higgs boson production and decay in the $H \to ZZ^* \to 4\ell$ and $H \to \gamma\gamma$ channels using $\sqrt{s} = 13$ TeV pp collision data collected with the ATLAS experiment*, Tech. Rep. ATLAS-CONF-2017-047, CERN, Geneva, 2017.

[15] K. Jakobs, G. Quast and G. Weiglein, *Higgs-Boson Physics at the LHC*, in *The Large Hadron Collider: Harvest of Run 1* (T. Schorner-Sadenius, ed.), pp. 195–258. Springer, Cham, 2015. DOI.

[16] S. Liebler, G. Moortgat-Pick and G. Weiglein, *Off-shell effects in Higgs processes at a linear collider and implications for the LHC*, *JHEP* **06** (2015) 093, [1502.07970].

[17] N. Greiner, S. Liebler and G. Weiglein, *Interference contributions to gluon initiated heavy Higgs production in the Two-Higgs-Doublet Model*, *Eur. Phys. J.* **C76** (2016) 118, [1512.07232].

[18] LHC Higgs Cross Section Working Group, A. David, A. Denner, M. Duehrssen, M. Grazzini, C. Grojean, G. Passarino et al., *LHC HXSWG interim recommendations to explore the coupling structure of a Higgs-like particle*, 1209.0040.

[19] LHC Higgs Cross Section Working Group, J. R. Andersen et al., *Handbook of LHC Higgs Cross Sections: 3. Higgs Properties*, 1307.1347. 10.5170/CERN-2013-004.

[20] R. Benbrik, M. Gomez Bock, S. Heinemeyer, O. Stål, G. Weiglein and L. Zeune, *Confronting the MSSM and the NMSSM with the Discovery of a Signal in the two Photon Channel at the LHC*, *Eur. Phys. J.* **C72** (2012) 2171, [1207.1096].

[21] P. Bechtle, S. Heinemeyer, O. Stål, T. Stefaniak, G. Weiglein and L. Zeune, *MSSM Interpretations of the LHC Discovery: Light or Heavy Higgs?*, *Eur. Phys. J.* **C73** (2013) 2354, [1211.1955].

[22] P. Bechtle, H. E. Haber, S. Heinemeyer, O. Stål, T. Stefaniak, G. Weiglein et al., *The Light and Heavy Higgs Interpretation of the MSSM*, *Eur. Phys. J.* **C77** (2017) 67, [1608.00638].

[23] P. Drechsel, L. Galeta, S. Heinemeyer and G. Weiglein, *Precise Predictions for the Higgs-Boson Masses in the NMSSM*, *Eur. Phys. J.* **C77** (2017) 42, [1601.08100].

[24] F. Domingo and G. Weiglein, *NMSSM interpretations of the observed Higgs signal*, *JHEP* **04** (2016) 095, [1509.07283].

[25] P. Bechtle, S. Heinemeyer, O. Stål, T. Stefaniak and G. Weiglein, *HiggsSignals: Confronting arbitrary Higgs sectors with measurements at the Tevatron and the LHC*, *Eur. Phys. J.* **C74** (2014) 2711, [1305.1933].

[26] P. Bechtle, S. Heinemeyer, O. Stål, T. Stefaniak and G. Weiglein, *Probing the Standard Model with Higgs signal rates from the Tevatron, the LHC and a future ILC*, *JHEP* **11** (2014) 039, [1403.1582].

[27] P. Bechtle, O. Brein, S. Heinemeyer, G. Weiglein and K. E. Williams, *HiggsBounds: Confronting Arbitrary Higgs Sectors with Exclusion Bounds from LEP and the Tevatron*, *Comput. Phys. Commun.* **181** (2010) 138–167, [0811.4169].

[28] P. Bechtle, O. Brein, S. Heinemeyer, G. Weiglein and K. E. Williams, *HiggsBounds 2.0.0: Confronting Neutral and Charged Higgs Sector Predictions with Exclusion Bounds from LEP and the Tevatron*, *Comput. Phys. Commun.* **182** (2011) 2605–2631, [1102.1898].

[29] M. Carena, S. Heinemeyer, O. Stål, C. E. M. Wagner and G. Weiglein, *MSSM Higgs Boson Searches at the LHC: Benchmark Scenarios after the Discovery of a Higgs-like Particle*, *Eur. Phys. J.* **C73** (2013) 2552, [1302.7033].

[30] H. Bahl, E. Fuchs, T. Hahn, S. Heinemeyer, S. Liebler, S. Patel et al., *MSSM Higgs Boson Searches at the LHC: Benchmark Scenarios for Run 2 and Beyond*, 1808.07542.

[31] S. Heinemeyer, W. Hollik and G. Weiglein, *The Masses of the neutral CP - even Higgs bosons in the MSSM: Accurate analysis at the two loop level*, *Eur.Phys.J.* **C9** (1999) 343–366, [hep-ph/9812472].

[32] S. Heinemeyer, W. Hollik and G. Weiglein, *FeynHiggs: A Program for the calculation of the masses of the neutral CP even Higgs bosons in the MSSM*, *Comput.Phys.Commun.* **124** (2000) 76–89, [hep-ph/9812320].

[33] G. Degrassi, S. Heinemeyer, W. Hollik, P. Slavich and G. Weiglein, *Towards high precision predictions for the MSSM Higgs sector*, *Eur.Phys.J.* **C28** (2003) 133–143, [hep-ph/0212020].

[34] M. Frank, T. Hahn, S. Heinemeyer, W. Hollik, H. Rzehak et al., *The Higgs Boson Masses and Mixings of the Complex MSSM in the Feynman-Diagrammatic Approach*, *JHEP* **0702** (2007) 047, [hep-ph/0611326].

[35] T. Hahn, S. Heinemeyer, W. Hollik, H. Rzehak and G. Weiglein, *High-Precision Predictions for the Light CP -Even Higgs Boson Mass of the Minimal Supersymmetric Standard Model*, *Phys. Rev. Lett.* **112** (2014) 141801, [1312.4937].

[36] H. Bahl and W. Hollik, *Precise prediction for the light MSSM Higgs boson mass combining effective field theory and fixed-order calculations*, *Eur. Phys. J.* **C76** (2016) 499, [1608.01880].

[37] H. Bahl, S. Heinemeyer, W. Hollik and G. Weiglein, *Reconciling EFT and hybrid calculations of the light MSSM Higgs-boson mass*, *Eur. Phys. J.* **C78** (2018) 57, [1706.00346].

[38] F. Domingo, P. Drechsel and S. Paßehr, *On-Shell neutral Higgs bosons in the NMSSM with complex parameters*, *Eur. Phys. J.* **C77** (2017) 562, [1706.00437].

[39] F. Domingo, S. Heinemeyer, S. Paßehr and G. Weiglein, *Decays of the neutral Higgs bosons into SM fermions and gauge bosons in the $\mathcal{CP}$-violating NMSSM*, 1807.06322.

[40] S. Paßehr and G. Weiglein, *Two-loop top and bottom Yukawa corrections to the Higgs-boson masses in the complex MSSM*, *Eur. Phys. J.* **C78** (2018) 222, [1705.07909].

[41] S. Borowka, S. Paßehr and G. Weiglein, *Complete two-loop QCD contributions to the lightest Higgs-boson mass in the MSSM with complex parameters*, *Eur. Phys. J.* **C78** (2018) 576, [1802.09886].

[42] J. Pardo Vega and G. Villadoro, *SusyHD: Higgs mass Determination in Supersymmetry*, *JHEP* **07** (2015) 159, [1504.05200].

[43] CMS Collaboration, A. M. Sirunyan et al., *Search for the Higgs boson decaying to two muons in proton-proton collisions at $\sqrt{s} = 13$ TeV*, 1807.06325. submitted to Phys. Rev. Lett.

[44] CMS Collaboration, A. M. Sirunyan et al., *Search for lepton flavour violating decays of the Higgs boson to $\mu\tau$ and $e\tau$ in proton-proton collisions at $\sqrt{s} = 13$ TeV*, *JHEP* **06** (2018) 001, [1712.07173].

[45] CMS Collaboration, V. Khachatryan et al., *Search for Lepton-Flavour-Violating Decays of the Higgs Boson*, *Phys. Lett.* **B749** (2015) 337–362, [1502.07400].

[46] CMS Collaboration, V. Khachatryan et al., *Search for lepton flavour violating decays of the Higgs boson to $e\tau$ and $e\mu$ in proton–proton collisions at $\sqrt{s} = 8$ TeV*, *Phys. Lett.* **B763** (2016) 472–500, [1607.03561].

[47] ATLAS Collaboration, *Searches for the $Z\gamma$ decay mode of the Higgs boson and for new high-mass resonances in pp collisions at $\sqrt{s} = 13$ TeV with the ATLAS detector*, *JHEP* **10** (2017) 112, [1708.00212].

[48] ATLAS Collaboration, *Search for new phenomena in high-mass diphoton final states using 37 fb^{-1} of proton–proton collisions collected at $\sqrt{s} = 13$ TeV with the ATLAS detector*, *Phys. Lett.* **B775** (2017) 105–125, [1707.04147].

[49] M. A. Ebert, S. Liebler, I. Moult, I. W. Stewart, F. J. Tackmann, K. Tackmann et al., *Exploiting jet binning to identify the initial state of high-mass resonances*, *Phys. Rev.* **D94** (2016) 051901, [1605.06114].

[50] Malte Hoffmann, *Search for the decay of a heavy Higgs boson decaying to two light Higgs bosons using a kinematic fit*, Ph.D. thesis, Universität Hamburg, 2016. http://ediss.sub.uni-hamburg.de/volltexte/2016/8244.

[51] CMS Collaboration, V. Khachatryan et al., *Searches for a heavy scalar boson H decaying to a pair of 125 GeV Higgs bosons hh or for a heavy pseudoscalar boson A decaying to Zh, in the final states with $h \to \tau\tau$*, *Phys. Lett.* **B755** (2016) 217–244, [1510.01181].

[52] CMS Collaboration, V. Khachatryan et al., *Search for neutral MSSM Higgs bosons decaying to a pair of tau leptons in pp collisions*, *JHEP* **10** (2014) 160, [1408.3316].

[53] CMS Collaboration, A. M. Sirunyan et al., *Search for additional neutral MSSM Higgs bosons in the $\tau\tau$ final state in proton-proton collisions at $\sqrt{s} = 13$ TeV*, 1803.06553. submitted to JHEP.

[54] CMS Collaboration, *Performance of reconstruction and identification of tau leptons in their decays to hadrons and tau neutrino in LHC Run-2*, Tech. Rep. CMS-PAS-TAU-16-002, CERN, Geneva, 2016.

[55] CMS Collaboration, V. Khachatryan et al., *Search for neutral MSSM Higgs bosons decaying into a pair of bottom quarks*, *JHEP* **11** (2015) 071, [1506.08329].

[56] CMS Collaboration, A. M. Sirunyan et al., *Search for beyond the standard model Higgs bosons decaying into a $\mathrm{b\bar{b}}$ pair in pp collisions at $\sqrt{s} = 13$ TeV*, *JHEP* **08** (2018) 113, [1805.12191].

[57] CMS Collaboration, V. Khachatryan et al., *Search for a very light NMSSM Higgs boson produced in decays of the 125 GeV scalar boson and decaying into τ leptons in pp collisions at $\sqrt{s} = 8$ TeV*, *JHEP* **01** (2016) 079, [1510.06534].

[58] E. Fuchs and G. Weiglein, *Impact of CP-violating interference effects on MSSM Higgs searches*, *Eur. Phys. J.* **C78** (2018) 87, [1705.05757].